Field driven ferromagnetic phase nucleation and propagation from the domain boundaries in antiferromagnetically coupled perpendicular anisotropy films

T. Hauet ,
San Jose Research Center, Hitachi Global Storage Technology, San Jose, CA 95135, USA

C. Günther
BESSY GmbH, 12489 Berlin, Germany

O. Hovorka, A. Berger
CIC nanoGUNE Consolider, E-20009 Donostia – San Sebastian, Spain

M.-Y. Im, P. Fischer
Center for X-Ray Optics, Lawrence Berkeley National Laboratory, Berkeley, CA 94720 USA

O. Hellwig
San Jose Research Center, Hitachi Global Storage Technology, San Jose, CA 95135, USA

We investigate the reversal process in antiferromagnetically coupled $[Co/Pt]_{X-1}/\{Co/Ru/[Co/Pt]_{X-1}\}_{16}$ multilayer films by combining magnetometry and Magnetic soft X-ray Transmission Microscopy (MXTM). After out-of-plane demagnetization, a stable one dimensional ferromagnetic (FM) stripe domain phase (tiger-tail phase) for a thick stack sample (X=7 is obtained), while metastable sharp antiferromagnetic (AF) domain walls are observed in the remanent state for a thinner stack sample (X=6). When applying an external magnetic field the sharp domain walls of the thinner stack sample transform at a certain threshold field into the FM stripe domain wall phase. We present magnetic energy calculations that reveal the underlying energetics driving the overall reversal mechanisms.

Strong perpendicular anisotropy Co/Pt multilayer systems that are antiferromagnetically coupled via thin Ru or NiO interlayers have recently been proposed as model systems to study the competition between local interlayer exchange and long-range dipolar interactions [1-4]. The observation of magnetic structure transformations induced by variation of extrinsic parameters such as an externally applied magnetic field provide the possibility to investigate the delicate energy balance in such systems [5-6]. So far, magnetic imaging experiments used mostly Magnetic Force Microscopy (MFM) for characterization, however, since this technique detects surface stray fields only and always exhibits some ambiguity due to strong tip/sample interactions [2,4,5] these results were not conclusive. .

In this letter, we present a study of the domain boundary structure in $[Co/Pt]_{X-1}/\{Co/Ru/[Co/Pt]_X\}_{16}$ AF-coupled multilayers. We report on magnetometry measurements and Magnetic Transmission X-ray Microscopy (MTXM) imaging of two different samples chosen to be on each side of the dipolar induced phase transition from sharp AF domain walls (X=6) to one-dimensional FM stripe domain walls (tiger-tails) (X=7) at remanence [2,5]. We explore the evolution of their remanent states in an external magnetic field and compare our experimental data with corresponding energy calculations.

The exact sample structure we use is $[Co(4Å)/Pt(7Å)]_{x-1}/\{Co(4Å)/Ru(9Å)/[Co(4Å)/Pt(7Å)]_{x-1}\}_{16}$ with X=6 and X=7, referred to as sample A and sample B respectively. The multilayers were deposited by DC magnetron sputtering onto X-ray transparent SiN_x membranes at ambient temperature. We use a commercial VSM to measure magnetization versus perpendicular-to-the-film field.

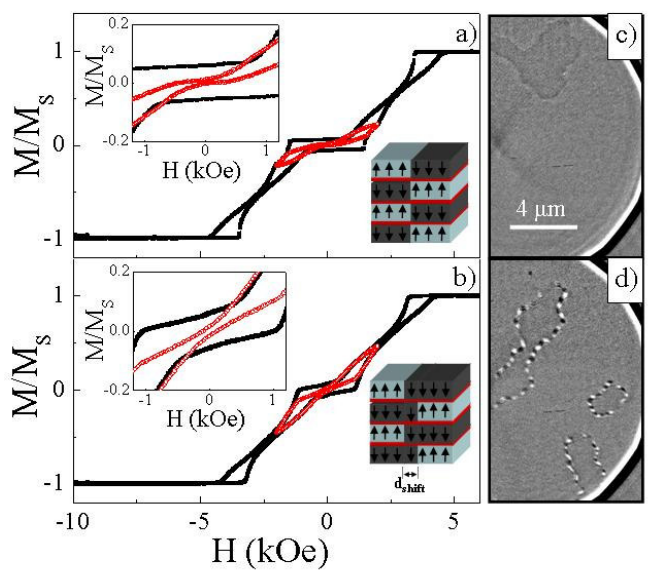

FIG. 1. Normalized magnetization as a function of field measured on sample A (a) and sample B (b) at 300 K. Solid symbols are the major loop measured between +/-10 kOe, while open symbols are a minor loop between +/-2 kOe after out-of-plane demagnetization. The insets show the range between +/- 1.2 kOe in more detail. c) and d) are MXTM images of the demagnetized state of sample A and B respectively showing AF domains with different domain wall structure.

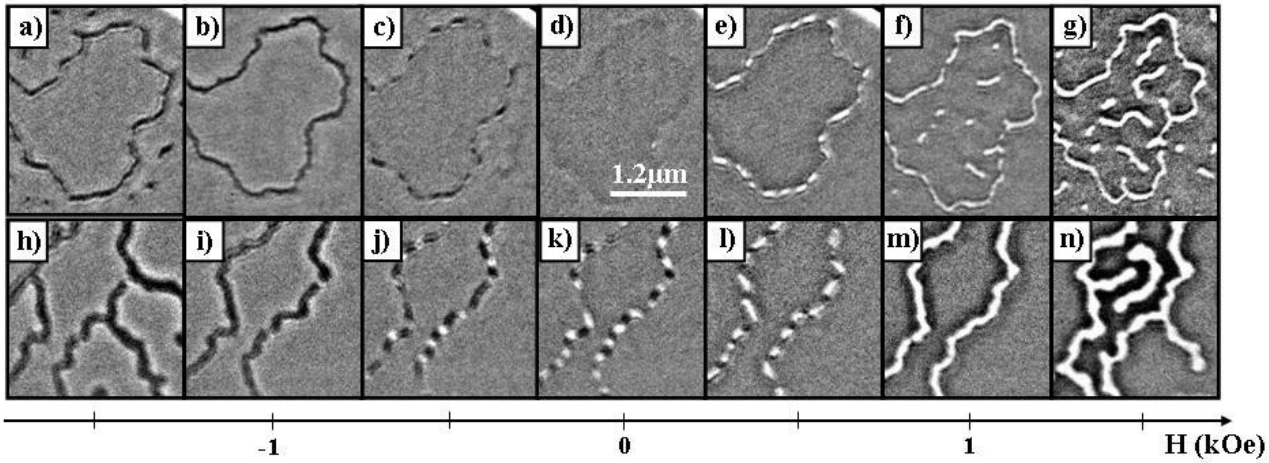

FIG. 2. MXTM images of sample A (a-g) and sample B (h-n) showing the magnetic domain configuration at -1.5 kOe (a,h), -1 kOe (b,i), -0.5 kOe (c,j), 0 Oe (d,k), 0.5 kOe (e,l), 1 kOe (f,m) and 1.5 kOe (g,n).

Fig. 1a shows hysteresis loops of sample A measured at 300 K. Starting from positive saturation, the first drop in magnetization corresponds to the synchronized reversal of 8 of the overall 17 Co/Pt stacks, such that the sample reaches a uniform AF state at remanence. Due to the odd number of stacks only one type of AF domain is populated, with the top and bottom stack remaining still in the previous saturation direction. When applying negative fields to the uniform AF remanent state we observe initially the reversal of the two surface stacks and then the 7 remaining bulk stacks switch in a second synchronized reversal. The corresponding behavior of sample B is similar (Fig. 1b) except that the surface stack reversal is less well visible [5].

To achieve a further microscopic understanding of this behaviour, we performed high-resolution MTXM experiments to image the domain structure of samples A and B close to the magnetic phase transition reported earlier [1,5]. Exploiting X-ray magnetic circular dichroism (XMCD) as strong and element-specific contrast mechanism, we use Fresnel zone plates as optical elements, which allow imaging lateral magnetic structures such as domains or domain walls with spatial resolution down to 15 nm [7,8]. Experiments were done at the Advanced Light Source in Berkeley, CA at beamline 6.2.1. [7,9]. Fig. 1c and 1d present remanent MXTM images measured at 300 K at the Co-L_3 absorption edge after out-of-plane demagnetization of samples A and B respectively. We observe a weak contrast between different AF domains due to the overall odd number of Co/Pt stacks, which prevents a perfect compensation of the magnetization. For the thinner stack sample A (Fig. 1c), we observe between the two regions of opposite AF order (up-down-up-… versus down-up-down-…) sharp AF domain walls as illustrated in the inset of Fig. 1a. Here the domain walls of the individual stacks are all vertically aligned with each other, thus minimizing the AF inter-stack exchange energy. The remanent magnetization is zero due to the 50/50 domain state as shown in the inset of Fig. 1a. This is no longer the case for the thicker sample B, which shows a non-zero magnetization (Fig. 1b) and a FM stripe domain wall type, i.e. the domain walls of each individual stack are alternately shifted with respect to each other, thus minimizing the dipolar energy (Fig. 1d). This one dimensional stripe pattern along the AF domain walls (tiger-tails) has recently been explained via internal dipolar fields that are present at the AF domain wall boundaries [2,5].

The strength of MTXM becomes apparent when applying external magnetic fields to the remanent stripe domain wall state of sample B (Fig. 2h-n). Stripe domains magnetized along the external field grow on expense of the oppositely magnetized domains until a uniform FM stripe along the AF domain boundary is obtained at about +/-1 kOe (Fig. 2i and 2m). The FM stripe width d_{shift} (inset in Fig. 1b) increases slightly with growing external field, from 160 nm at remanence to 200 nm at 1 kOe. On the contrary, when applying external magnetic fields to sample A (Fig. 2a-f), sharp domain walls are preserved until about 250 Oe. Above this value new domains of much stronger contrast appear along the domain boundary (Fig. 2c and 2e) indicating the formation of FM order [2,5]. The FM phase nucleates all along the AF domain wall until a continuous FM ring is formed (Fig. 2b and 2f). Individual domain walls of each sub-layer stack are no longer vertically aligned, but exhibit an alternating shift to the left and to the right with respect to the zero field domain wall position. We find that d_{shift} is about 120 nm at 0.5 kOe.

To gain further insight into the differences between sample A and B, we calculate energy profiles of the AF domain wall structure as a function of d_{shift} as well as external field strength. The domain wall in each Co/Pt stack was assumed to be a Bloch-type wall with a fixed width of 25 nm [10]. Calculation details and parameter values can be found in Refs. [1,5]. Fig. 3a and 3b show the total energy profiles for the X=6 and X=7 sample at different applied field. In both cases, two energy minima are observed in remanence. The first minimum is located at d_{shift} = 0 nm and corresponds to vertically aligned sub-stack domain walls. The second energy minimum at a non-zero $d_{shift} = d^0_{shift}$ represents a FM domain boundary phase. In both cases, for X=6 and X=7, the second energy minimum is lower than the first one. However at zero field the second minima of sample B is about twice as low

if compared to sample A (inset Fig. 3a and 3b), thus revealing why the tiger-tail phase is more likely to develop in sample B (Fig. 2k), while the thinner sample is still trapped in the meta-stable no-shift phase (Fig. 2d). As the field increases, the energy of the second minima as well as the energy barrier (Fig. 3c) between the two minima are lowered with respect to the first minimum, while d^0_{shift} is slowly increasing (Figs. 3a and 3b). At 0.5 kOe, the energy barrier is annihilated for the X=6 sample. However, for sample A the observation of FM boundary domain nucleation below this threshold indicates the importance of thermal activation in this process. Note that the above scenario is reflected on a macroscopic scale. The minor loop slope around zero field (Fig. 1b) is much higher for sample B, consistent with the fact that this sample does not have to undergo a first order phase transition to produce a significant field response.

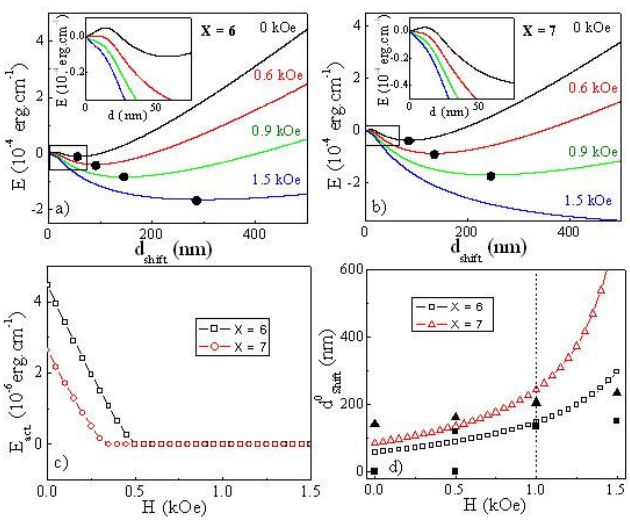

FIG. 3. a-b) Calculated total energy density for an AF domain wall as a function of the FM width d_{shift} for X =6 (a) and X=7 (b) for different field values as indicated. Inset: Close up of the region with small d_{shift}. Black dots are a guide to the eye for the energy minimum position. c) Energy barrier height with respect to first energy minimum as a function of field. d) Calculated optimum d^0_{shift} as a function field (open symbol) compared with FM domain widths extracted from Fig.2 (full symbols).

Finally, beyond 1 kOe, both samples, A and B, behave similarly. The FM boundary broadens, i.e. d_{shift} increases, and additional FM domains nucleate and propagate into the AF regions. In previous publications with only a few magnetic stacks, i.e. significantly lower dipolar interaction, a continuous widening of the FM domain boundary phase was observed towards saturation [3,4]. Here for a large stack number, dipolar fields prevent FM domain growth beyond a certain characteristic stripe domain width. For both samples, the overall odd number of Co/Pt stacks favors nucleating all-up domains inside one of the two AF domain regions since the Zeeman energy is slightly lower for that state. We obtain good agreement between the calculated and measured d_{shift} for fields up to 1 kOe as shown in Fig. 3d. For higher fields, experimentally d_{shift} increases slowly, and does not show the exponential expansion of the calculated d^0_{shift} values (Fig. 3d), since our 1D model cannot describe the formation of labyrinth stripe domains. Experimentally, further consequent widening only occurs after reaching 50% of the FM phase around 2.5 kOe.

In conclusion, we reveal details of the domain evolution in two thick $[Co/Pt]_{X-1}/\{Co/Ru/\ [Co/Pt]_{X-1}\}_{16}$ multilayers after out-of-plane demagnetization. We use MXTM to image the AF domain boundary structure in external magnetic fields. For X=7 we observe a stable "tiger-tail" pattern at remanence, while for X=6 a metastable sharp AF domain wall structure is preferred. These observations confirm previous analytical calculations [11]. In addition above a certain threshold field we observe nucleation of the FM phase all along the sharp AF domain boundary of the thinner of the two samples. Additional calculations elucidate the reversal behavior and the delicate energy balance of perpendicular AF-coupled multilayer systems in external magnetic fields.

Acknowledgments: We thank E. E. Fullerton and B. D. Terris for helpful discussions. This work was partially supported by Lavoisier fellowship. The soft X-ray microscope was supported by the Director, Office of Science, Office of Basic Energy Sciences, Materials Sciences and Engineering Division, of the U.S. Department of Energy. Work at nanoGUNE is supported by the Department of Industry, Trade and Tourism of the Basque Government and the Provincial Council of Gipuzkoa under the ETORTEK Program, Project IE06-172, as well as from the Spanish Ministry of Science and Education under the Consolider-Ingenio 2010 Program, Project CSD2006-53.

References

[1] O. Hellwig, T.L. Kirk, J.B. Kortright, A. Berger, and E.E. Fullerton, Nat. Mater. 2, 112 (2003).
[2] O. Hellwig, A. Berger, E.E. Fullerton, Phys. Rev. Lett. 91, 197203 (2003).
[3] A. Baruth et al., Appl. Phys. Lett. 89, 202505 (2006).
[4] Y. Fu et al., Appl. Phys. Lett. 91, 152505 (2007).
[5] O. Hellwig, A. Berger, J.B. Kortright, E.E. Fullerton, J. Magn. Magn. Mater. 319, 13 (2007).
[6] K. Janicka, J.D. Burton and E.Y. Tsymbal, J. Appl. Phys. 101, 113921 (2007).
[7] P. Fischer et al., Materials Today 9 (1-2), 26 (2006).
[8] W. Chao, B.H. Harteneck, J.A. Liddle, E.H. Anderson and D.T. Attwood, Nature (London) 435, 1210 (2005).
[9] P. Fischer, Current Opinion in Solid State and Materials Science, 7, 173 (2003).
[10] O. Hellwig, G.P. Denbeaux, J.B. Kortright, Eric E. Fullerton, Physica B 336, 136 (2003)
[11] N.S. Kiselev, I.E. Dragunov, U.K. Rossler, and A.N. Bogdanov, Appl. Phys. Lett. 91, 132507 (2007)

This work was supported by the Director, Office of Science, Office of Basic Energy Sciences, of the U. S. Department of Energy under Contract No. DE-AC02-05CH11231.